EPJ Web of Conferences **40**, 15012 (2013)
DOI: 10.1051/epjconf/20134015012

The effect of film thickness on the magnetic and magneto-transport properties of Sr_2FeMoO_6 thin films

Minnamari Saloaro[a], Sayani Majumdar, Hannu Huhtinen, and Petriina Paturi

Wihuri Physical Laboratory, Department of Physics and Astronomy, FI-20014 University of Turku, Finland

Abstract. Magnetoresistive Sr_2FeMoO_6 thin films were grown by pulsed laser deposition with three different thicknesses 150 nm, 270 nm and 500 nm. Structural, magnetic and magneto-transport properties of the films were measured. Structural properties showed that impurity phases are formed when the film thickness exceed limiting thickness over 300 nm. Otherwise no major differences were observed in structural and magnetic properties between the films. The semiconductive upturn was observed in all $\rho(T)$ curves, but it was notably smaller for the two thickest films. At 350 K the magnetoresistive (MR) behaviour was very similar for all the films, but at 10 K the negative MR was clearly largest for the thickest film and also the shape of the curve in low fields deviated from others.

1 Introduction

Double perovskite Sr_2FeMoO_6 (SFMO) is an extremely interesting material having high potential for spintronic and magnetoresistive applications. It is half-metallic resulting in 100 % spin polarized charge carriers and it has one of the highest Curie temperatures, T_C, among half metals, around 410-450 K [1–4]. In order to reach applications which operate at room temperature, the fabrication of high quality thin films with T_C clearly over room temperature is necessary. Even though the properties of SFMO are excellent for these applications, the fabrication of SFMO thin films has proven to be difficult [5–7]. The challenges in the SFMO thin film fabrication are due to extreme preparation conditions and easily formed impurity phases [5,6,8–10]. The best method to achieve pure and fully textured SFMO films has proven to be pulsed laser deposition (PLD) [5,6,11], because it does not require such a high vacuum and a stoichiometric target can be used. Earlier we have reported SFMO thin films with no indication of different orientations or impurity phases made with PLD in $Ar/H_2(5\%)$ atmosphere and at 1050°C deposition temperature [5]. More commonly used deposition atmosphere is oxygen [8,11–13], but it has been shown that an oxygen backround pressure higher than 10^{-4} mbar leads to impurity phases [8].

In addition to impurities, the anti-site disorder (ASD), where Fe and Mo transpose their positions in the lattice, together with possible oxygen vacancies have a strong deteriorating effect on the magnetic properties of the SFMO thin films [14–16]. Both ASD and oxygen vacancies narrow the band gap in the majority spin up band until at higher concentrations the half-metallic feature of SFMO electronic structure is lost [16–18]. ASD is easily formed in thin film samples and it is strongly related to the strain of SFMO film [7]. This could be the reason for the earlier observed change in the T_C between polycrystalline and thin film samples. It has been shown that polycrystalline target used in deposition has T_C around 400 K, while the T_C of thin films made of this target is at most 375 K [5]. Often the T_C's of polycrystalline samples are quite close to the theoretical T_C value 410-450 K, but in thin film samples the T_C does not usually reach as high values.

Earlier investigations have shown that the T_C of $La_{0.7}Sr_{0.3}MnO_3$, which has similar half-metallic properties as SFMO, is decreased in thinner samples and the magnetic properties are strongly related to the strain caused by the mismatch between the sample and the substrate [19]. The saturation magnetization of Sr_2FeMoO_{6+x} thin film has been seen to increase with increasing thickness, when $SrTiO_3$ (STO), $LaAlO_3$ and MgO substrates are used [20]. The saturation magnetization, however, remains constant with varying thicknesses when $Sr_{0.5}Ba_{0.5}TiO_3$ substrate, which has the best match with SFMO, is used [20]. The temperature dependence of resistivity in Sr_2FeMoO_{6+x} films is strongly dependent on the choice of substrate and the film thickness [20]. It has been found that the temperature dependence of resistivity in SFMO films grown on STO changes dramatically when the film thickness is under 66 nm and when the thickness is over 120 nm the typical low temperature upturn is seen in resistivity behaviour [20]. Also the surface roughness increases with increasing thickness [21].

Only few studies have been published about the effect of film thickness on the structural, magnetic and transport properties of SFMO thin films and the published results do not show consistency. Fix *et al.* [22,23] have obtained pseudomorphic epitaxial growth in SFMO films on STO substrate when the film thickness is less than 50 nm and fully relaxed films when the thickness is larger than 80 nm. Our earlier results [5] and results from Boucher *et al.* [21], however, do not show pseudomorphic growth nor fully relaxed film even at thicknesses over 100 nm. One of the problems that needs to be solved before fabrication of SFMO based multilayer structures, is to improve T_C and other magnetic properties that are reduced from bulk samples and at the same time not compromising the surface roughness. Because it has been observed in $La_{0.7}Sr_{0.3}MnO_3$ thin films that the magnetic properties improve with incresing thickness [19], it will be very in-

[a] e-mail: minnamari.saloaro@utu.fi

teresting to find out the effect of film thickness in case of SFMO.

In this paper, we have fabricated SFMO thin films with different thicknesses at optimized deposition temperature and atmosphere. We have clarified the effect of film thickness and the strain caused by the lattice mismatch on the structural, magnetic and magneto-transport properties of SFMO thin films.

2 Experimental methods

The SFMO thin films were deposited with pulsed laser deposition on the $SrTiO_3$ (001) single crystal substrate. Films were made in Ar/H_2(5%) atmosphere in 9.5 Pa pressure and the deposition temperature has been 1050°C. The deposition is described in detail in ref. [5]. The films were made with three different pulse numbers: 2000 (S2), 4000 (S4) and 8000 (S8) leading to thickness of 150 nm, 270 nm and 500 nm as measured by AFM profilometry. Structural characterization were done with X-ray diffraction (XRD) and atomic force microscopy (AFM). XRD measurements were carried out with Philips X'pert Pro MPD diffractometer using a Schulz texture goniometer. The phase purity, orientation, lattice parameters and the strain of the films were determined from θ-2θ-scans, texture measurements and 2θ-ϕ-scans. Texture of the films were measured for the SFMO (204) peaks (2θ = 57.16°) and typical impurity phase Fe (110) peaks (2θ = 44.98°) and $SrMoO_4$ (112) peaks (2θ = 27.68°). The AFM was used to determine the surface structure and the root mean square (RMS) roughness of the films.

Magnetic and magneto-transport properties of the films were determined with a SQUID magnetometer and Quantum Design Physical Property Measurement System (PPMS). SQUID magnetometer was used to determine the magnetization curves, $M(T)$, in 0.1 T magnetic field, which was in parallel with the plane of the films, and these curves were used to determine the T_C of the samples. The temperature dependence of resistivity was measured in 0 T, 50 mT, 100 mT, 500 mT, 1 T and 5 T fields with PPMS. Magnetoresistance between -8 T and 8 T fields was also measured with PPMS at 10 K and at range of 50-350 K with 50 K steps. The external field was perpendicular to the plane of the films during these measurements.

3 Results and discussion

3.1 Structural and magnetic properties

According to the XRD results, the S2- and S4-films are phase-pure and fully textured. The θ-2θ-scans did not show any impurity phases and only SFMO (00l) peaks for these two thinner films, but the detail of the θ-2θ-scans shown in Fig. 1 reveals impurity phase peak near 50° for S8-film. Similar impurity phase peak is also observed in S8-film at around 25° and these cannot be identified to any typical impurity of SFMO, but could indicate presence of Fe_2O_3. Because the Fe_2O_3 is weakly magnetic, it could not be detected with any magnetic or magneto-transport measurements. The SFMO pole figures however show only clear (204) and (132) peaks and no texture in the impurity phase

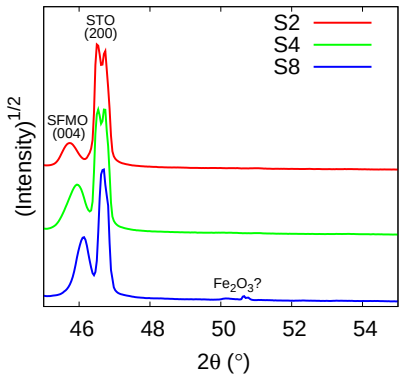

Fig. 1. Detail of the θ-2θ-scans between 45° and 55°.

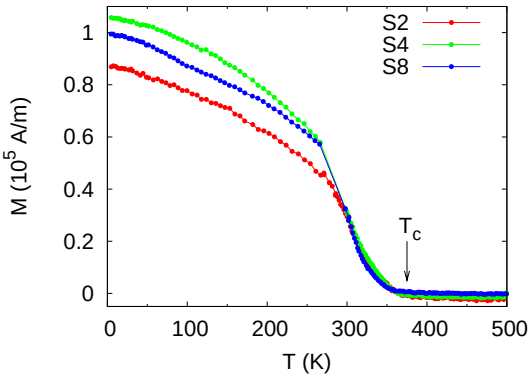

Fig. 2. Temperature dependences of magnetization for all the films in 100 mT field. The measurement were carried out in two parts from 5 K to 275 K and from 300 K to 500 K with different measuring configurations. This enables the use of the wide temperature range, but causes the lack of measuring points near 300 K.

pole figures as expected for fully textured c-axis oriented film. The lattice parameters a and c were determined from the θ-2θ- and 2θ-ϕ-scans. The a parameters are 5.532 Å, 5.610 Å and 5.595 Å for S2, S4 and S8 respectively. Correspondingly the c parameters are 7.952 Å, 7.928 Å and 7.904 Å. Compared to the lattice parameters of the target used in deposition (a = 5.587 Å and c = 7.970 Å [5]), the a is approximately equal in S4 and S8 films, but smaller in S2 film and the c is smaller in all the films. At the same time the lattice parameter a of the thinnest film is closest to the corresponding diagonal of STO substrate (5.52 Å). When the film thickness increases the parameter c decreases and the parameter a increases from S2 to S4 but is approximately same in S4 and S8 films. The changes in volume of the unit cell, $\Delta V = V_{film} - V_{target}$, are however rather small from 0.73 $Å^3$ for S4 to -1.35 $Å^3$ for S8 and -5.42 $Å^3$ for S2.

The 2θ-ϕ-scans of the SFMO (204) peak was used to determine the 2θ and ϕ full width at half maximum (FWHM) at the peak. The 2θ FWHM values increases with increasing thickness being 0.50° (S2), 0.63° (S4) and 0.75° (S8). When the 2θ instrumental width is 0.3°, it is clear that all the films have variation in the volume of the unit cell and the distribution of the unit cell volume through the film increases with increasing thickness. This, together with the

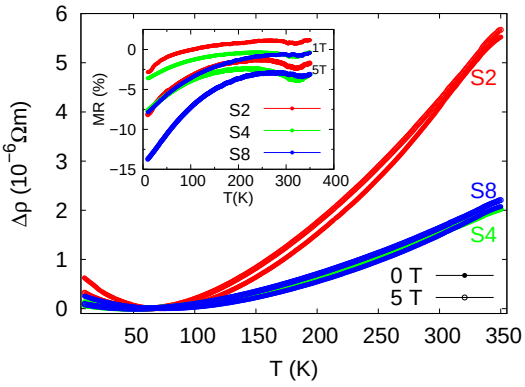

Fig. 3. Temperature dependence of the resistivity change for all the films in 0 T and 5 T magnetic fields. The inset shows the temperature dependence of magnetoresistance for all the films in 1 T and 5 T magnetic fields.

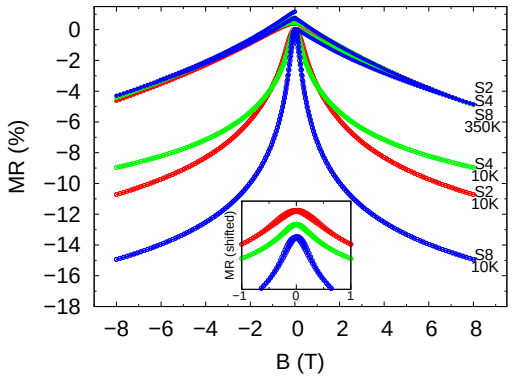

Fig. 4. Magnetic field dependence of magnetoresistance for all the samples at 350 K and 10 K. The inset shows the detail of the curves at 10 K and in low magnetic fields. The curves in the inset are shifted from each other in order to see the different shape of the curves in low magnetic field range.

lattice parameter values, means that the thinnest S2 film is most strained and the strain decreases when the thickness increases. The ϕ FWHM values are 0.64° (S2), 0.65° (S4) and 0.72° (S8) and the ϕ instrumental width is 0.3°. This indicates the presence of low angle grain boundaries in all the films, but the amount of these boundaries is quite low until some critical thickness over 270 nm is reached.

RMS-roughnesses were determined as an average of AFM image taken with 5 × 5 μm^2, 10 × 10 μm^2 and 20 × 20 μm^2 scans. The RMS-roughness of the S2-film is 14.00 nm, for the S4 film it is 15.87 nm and for S8-film 17.21 nm. All the values are quite close to each other, but a slight increase in RMS-roughness with increasing thickness is observed. The RMS-roughness values are also quite high compared to the previously obtained values (from 2.7 nm to 9.7 nm [5,24]) and considering the possible multilayer structured applications. The film thickness was determined with AFM over an edge etched with nitric acid. The thickness is 150 nm for S2-film, 270 nm for S4-film and for S8-film 500 nm.

The temperature dependence of field-cooled (FC) magnetization is shown in Fig. 2. The Curie temperature T_C was determined from the curves at the point where the magnetization deviates from the minimum and the point is shown with an arrow in Fig. 2. Only slight changes in the T_C were observed between samples. The T_C of the S2-film is 380 K, for the S4-film the T_C is 378 K and it is 372 K for S8-film. Thus, the T_C appears to slightly decrease with increasing thickness. Because of the uncertainties in film thickness and area measurements the magnetisation of all the films at 5 K are approximately same within the error limits. Therefore, we can conclude that the magnetic properties do not significantly change in SFMO films with different thicknesses, but after some threshold thickness, over 300 nm, an impurity phase is formed.

3.2 Magneto-transport properties

Change of the resistivity in regard to minimum of the resistivity, $\Delta\rho = \rho(T) - \rho_{min}$, as a function of temperature is shown in Fig. 3 for all the films. The curves show metallic behaviour at temperatures over 75 K and at lower temperatures a small upturn, indicating semiconductive behaviour, is seen. The resistivity behaviour of two thicker S4- and S8-films are very similar, but differ dramatically from the resistivity behaviour of the thinnest S2-film. For the S2-film, the upturn is clearly largest as also the change in the resistivity. The zero field resistivity at 10 K is 8.3 $\mu\Omega$m for S2-film, which is also remarkably larger than the values 2.7 $\mu\Omega$m for S4-film and 3.3 $\mu\Omega$m for S8-film. Earlier investigations have shown that the strain reduces the band gap in the majority spin band [22], which makes the excitation of the electron to the conduction band easier and that way enables the SFMO film behave as a system with semiconductive majority spin band. The XRD results showed, the S2-film is more strained than the thicker films, which could explain the greater semiconductive upturn in $\Delta\rho$ curve of S2-film. The resistivity-minimum temperatures ($T_{\rho-min}$) were determined from the temperature derivative of the resistivity as an average of the values in different magnetic fields. For S2- and S8-films the $T_{\rho-min}$ was around 68 K and for S4-film around 59 K. The variation of the $T_{\rho-min}$ values in magnetic field was however clearly greater in S8-film, while it was approximately same for S2- and S4-films.

Fig. 4 shows the magnetoresistance (MR% = $(R_B - R_0)/R_0 \times 100$) of the films at 350 K and 10 K, while the inset shows the detail of the 10 K curves in low magnetic field. At 350 K, where the ferromagnetic interaction is already quite weak, all the films show very similar magnetoresistive behaviour. At 10 K negative magnetoresistance is obviously largest around 15% for the thickest S8-film and also the shape of the curve for S8-film differs from others especially in the low field part. The negative magnetoresistance of S2- and S4-films are more similar, even though the MR% is around -11 for S2-film and -9 for S4-film. Because the shape of the curves in Fig. 4 changes between the samples especially in low fields, it gives indication that the same magneto-transport mechanism is not dominant in all the films. Our earlier investigation have also shown that the MR in SFMO thin films cannot be explained with any common MR mechanism [25]. The temperature dependence of magnetoresistance in 1 T and 5 T magnetic fields is shown in the inset of Fig. 3. The magnetoresistive behaviour is quite similar for all the films at higher temperatures and MR% decreases with decreas-

ing temperature. The decrease is however more rapid for S8-film and this corresponds very well to the change of MR in fields seen in Fig. 4. At higher temperatures above 300 K, a local minimum is observed in all the curves in the inset of Fig. 3. Most likely this minimum is related to the ferro-paramagnet transition, since it occurs around the same temperature where the midpoint of the transition is.

The magnetic properties of the films were very similar and the largest differences in the structure between the films were the strain and the amount of low angle grain boundaries. Therefore, the differences seen in the magneto-transport properties of films with different thicknesses are most likely related to relaxation of the films and to the presence of these grain boundaries. The strain is closely related to the formation of ASD [7], which also increases the zero field resistivity of the films. The strain was highest in the thinnest S2-film where also the zero field resistivity was largest. This gives the impression that the S2-film has more ASD than the thicker films. Eventhough the ASD normally increases the magnetoresistivity, recent results show that if the amount of ASD is high enough, which shows as increased zero field resistivity, the MR is reduced [26,27]. This could possibly explain the larger negative MR observed in thickest S8-film. The changes in the shape of the curves in Fig. 4 could be related to tunneling type MR accross the low angle grain boundaries, which would be enhanced in S8 film due to the observed increase of these boundaries. Considering the magnetoresistive sensor applications the large MR effect observed in S8-film is desired, but for spintronic applications the spin polarization and the magnetic properties are more important. Both S4- and S8-films have quite good and similar magnetic properties and according to the resistivity measurements higher spin polarization than the S2-film. This suggests that thickness around 500 nm is promising for magnetoresistive applications, but for spintronic applications the film thickness around 270 nm is at least as good.

4 Conclusion

In summary, we have investigated the properties of SFMO thin films with different thicknesses. The structural properties showed impurity phases and an increase in the amount of low angle grain boundaries, when the thickness exceeds some limiting value, over 300 nm. The relaxation of the films increases with increasing thickness and only slight changes in the unit cell volumes were observed. A slight decrease in T_C with increasing thickness was observed. In thinnest 150 nm film the semiconductive upturn in $\rho(T)$-curve is clearly seen, while in thicker 270 nm and 500 nm films it is smaller. The negative MR was observed in all the films and it was largest at 10 K in the thickest film. For magnetoresistive applications the thickness around 500 nm seems promising with the highest MR effect, but for spintronic applications the thickness around 270 nm seems at least as good with good magnetic properties and high spin polarization. The observed formation of impurity phases anyhow limits the usable film thickness to around 300 nm. The roughness of these films were so large that they can not be used in multilayers structures. Therefore, more optimization, especially with the medium thickness film, is needed before fabrication of SFMO multilayer structures for applications.

References

1. K.I. Kobayashi, T. Kimura, H. Sawada, K. Terakura, Y. Tokura, Nature **395**, 677 (1998)
2. D.D. Sarma, P. Mahadevan, T. Saha-Dasgupta, S. Ray, A. Kumar, Phys. Rev. Lett. **85**, 2549 (2000)
3. J. Rager, A.V. Berenov, L.F. Cohen, W.R. Branford, Y.V. Bugoslavsky, Y. Miyoshi, M. Ardakani, J.L. MacManus-Driscoll, Appl. Phys. Lett. **81**, 5003 (2002)
4. C.L. Yuan, Y. Zhu, P.P. Ong, C.K. Ong, T. Yu, Z.X. Shen, Physica B **334**, 408 (2003)
5. P. Paturi, M. Metsänoja, H. Huhtinen, Thin Solid Films **519**, 8047 (2011)
6. T. Suominen, J. Raittila, P. Paturi, Thin Solid Films **517**, 5793 (2009)
7. D. Kumar, D. Kaur, Physica B **405**, 3259 (2010)
8. A. di Trolio, R. Larciprete, A.M. Testa, D. Fiorani, P. Imperatori, S. Turchini, N. Zema, J. Appl. Phys. **100**, 013907 (2006)
9. W. Westerburg, D. Reisinger, G. Jakob, Phys. Rev. B **62**, R767 (2000)
10. J. Santiso, A. Figueras, J. Fraxedas, Surf. Interface Anal. **33**, 676 (2002)
11. T. Manako, M. Izumi, Y. Konishi, K.I. Kobayashi, M. Kawasaki, Y. Tokura, Appl. Phys. Lett. **74**, 2215 (1999)
12. S.R. Shinde, S.B. Ogale, R.L. Greene, T. Venkatesan, K. Tsoi, S.W. Cheong, A.J. Millis, J. Appl. Phys. **93**, 1605 (2003)
13. A. Venimadhav, F. Sher, J.P. Attfield, M.G. Blamire, J. Magn. and Magn. Mater. **269**, 101 (2004)
14. B.J. Park, H. Han, J. Kim, Y.J. Kim, C.S. Kim, B.W. Lee, J. Magn. and Magn. Mater. **272-276**, 1851 (2004)
15. B. Aguilar, O. Navarro, M. Avignon, Microelectronics Journal **39**, 560 (2008)
16. D. Stoeffler, S. Colis, J. Phys. Cond. Mat. **17**, 6415 (2005)
17. T. Saha-Dasgupta, D.D. Sarma, Phys. Rev. B **64**, 064408 (2001)
18. D. Stoeffler, S. Colis, J. Magn. and Magn. Mater. **290-291**, 400 (2005)
19. L. Ranno, A. Llobet, R. Tiron, E. Favre-Nicolin, Applied Surface Science **188**, 170 (2002)
20. R. Boucher, J. Magn. and Magn. Mater. **301**, 251 (2006)
21. R. Boucher, Journal of Physics and Chemistry of Solids **66**, 1020 (2005)
22. T. Fix, D. Stoeffler, S. Colis, C. Ullhaq, G. Versini, J.P. Vola, F. Huber, A. Dinia, J. Appl. Phys. **98**, 023712 (2005)
23. T. Fix, G. Versini, J.L. Loison, S. Colis, G. Schmerber, G. Pourroy, A. Dinia, J. Appl. Phys. **97**, 024907 (2005)
24. M. Metsänoja, S. Majumdar, H. Huhtinen, P. Paturi, J Supercond Nov Magn **25**, 829 (2012)
25. M. Saloaro, S. Majumdar, H. Huhtinen, P. Paturi, J. Phys. Cond. Mat. **24**, 366003 (2012)
26. D. Sánchez, M. García-Hernández, N. Auth, G. Jakob, J. Appl. Phys. **96**, 2736 (2004)
27. V.N. Singh, P. Majumdar, Europhys. Lett. **94**, 47004 (2011)